A Semiempirical PM3 Treatment of Benzotetrazepinone Decomposition in Acid Media

C. I. Williams and M. A. Whitehead*

Theoretical Chemistry Laboratory, Department of Chemistry, McGill University, 801 Sherbrooke Street West, Montreal, Quebec, Canada H3A 2K6

Bertrand J. Jean-Claude

Department of Oncology, McGill University, 3655 Drummond Street, Ste. 701, Montreal, Quebec, Canada H3G 1Y6

Received February 7, 1997 (Revised Manuscript Received June 26, 1997[⊗]*)*

A mechanism for benzotetrazepinone (BTZ) ring opening in acid media is proposed and investigated with the semiempirical PM3 method. The PM3 energies predict the experimentally observed effect of aryl-ring substituents on the pH of tetrazepinone ring opening. Linear free energy reaction constants ($\rho = 3.36$ and $\rho^+ = 2.25$) for the internal cyclization of *N*-(2-diazoniumphenyl)-*N*-methyl-*N*′-methyl ureas (DPMU) to BTZs are calculated by relating PM3 enthalpy differences to aryl-ring substituent Hammett constants σ and σ^+. The pK_a of a protonated benzotetrazepinone is estimated to be −1.0, which is similar to experimental pK_a's of structurally analogous benzamides and phenylureas. Experimental percent yields of various tetrazepinones are correlated with PM3 energy differences. The PM3 method is also used to explain why some DPMUs cyclize to *N*-carbamoylbenzotriazoles (NCBT) instead of BTZs.

Introduction

Benzotetrazepinones **1** (BTZ) represent a relatively new class of compounds which contain the novel seven-membered tetrazepinone ring system.[1] Tetrazepinones show significant cytotoxic activity in alkylating-agent resistant tumor cells.[2]

The only known synthetic route for synthesis of benzotetrazepinones is through the internal cyclization of *N*-(2-diazoniumphenyl)-*N*-methyl-*N*′-methyl ureas **2** (DPMU)[1,3] (Figure 1). Pyridotetrazepinones (**1l**, Figure 2), tricyclic tetrazepinones (**1m**, Figure 2), and a number of aryl ring substituted benzotetrazepinones (**1a**−**d**, Figure 2) have been synthesized by this route,[1,3] but attempts to synthesize benzotetrazepinones with H as the N5 substituent (**1n**) fail, because irreversible cyclization to *N*-carbamoylbenzotriazole **3** (NCBT) occurs instead (Figure 1).[3]

Benzotetrazepinone stabilities and synthetic percent yields are markedly influenced by their aryl ring substituents.[3] For example, *p*-nitro-BTZ **1c** is synthesized in good yields (>80%) and is sufficiently stable for X-ray structural determination, while *p*-methoxy-BTZ **1b** is obtained in lower yields (<40%), and readily decomposes to methyl isocyanate and benzotriazole **4**, Figure 3.[3] UV/vis and ^{15}N NMR data suggest that benzotetrazepinones undergo a retrosynthetic ring opening to their DPMU precursors[3,4] in aqueous acid, at a pH which depends upon their aryl ring substituents. In an aqueous solution of pH = 4, *p*-methoxy-substituted BTZ **1b** is 100% in the ring open form **2**, while *p*-nitro-BTZ **1c** is only 40% in the ring open form. No experimental pK_a's or Hammett reaction constants exist for tetrazepinones.

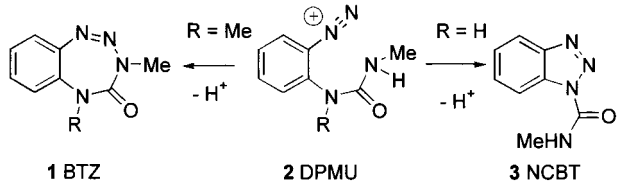

Figure 1. Tetrazepinone synthesis (only DPMU with R = Me cyclize to tetrazepinones).

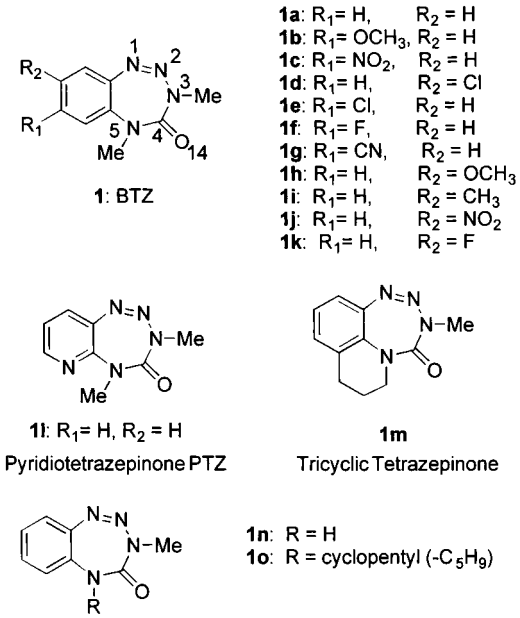

Figure 2. Representative tetrazepinones.

The development of tetrazepinones as antitumor agents would undoubtedly be hastened if computational approaches could be used to help elucidate tetrazepinone decomposition mechanisms and to predict the properties and reactivities of new tetrazepinone drug candidates prior to their synthesis. Computational methods will be used here to study tetrazepinone decomposition mecha-

[⊗] Abstract published in *Advance ACS Abstracts,* August 1, 1997.

(1) Jean-Claude, B. J.; Just, G. *J. Chem. Soc., Perkin Trans. 1* **1991**, 2525.
(2) Jean-Claude, B. J.; Mustafa, A.; Cetateanu, N. D.; Damian, D.; de Marte, J.; Yen, R.; Vasilescu, D.; Chan, T. H.; Leyland-Jones, B. *Br. J. Cancer*, in press.
(3) Jean-Claude, B. J. Ph.D. Thesis, McGill University, 1992.
(4) Jean-Claude, B. J.; Williams, C. I. *Magn. Reson. Chem.*, in press.

S0022-3263(97)00225-9 CCC: $14.00

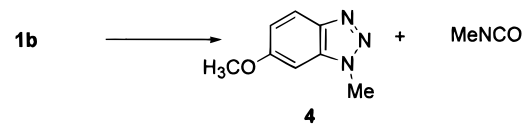

Figure 3. Decomposition of BTZ **1b** into benzotriazoles (**4**) and methyl isocyanate.

nisms and to quantify trends in existing experimental data. Specifically, this work investigates (a) the possible mechanisms of acid-induced BTZ ring opening, (b) the effect of aryl ring substituents on the acid-induced BTZ ring opening to DPMU, (c) the effect of aryl ring substituents on the formation of BTZs from DPMU, (d) the effect of aryl ring substituents on BTZ synthetic yields, and (e) the formation of NCBT instead of BTZ from DPMU with R = H as the N5 substituent.

The PM3[5] method was used exclusively in this study because semiempirical methods,[6−23] and the PM3 method in particular,[24−32] have proven accurate for predicting numerous other nitrogen heterocyclic properties. Previous theoretical work has shown PM3 to be the best semiempirical method for reproducing benzotetrazepinone X-ray geometries.[33] Computer constraints precluded using *ab initio* methods for all the reactants, products, intermediates and transition states considered here, but *ab initio* calculations (3-21G*, 6-31G**) were performed in some cases to compare with the PM3 results. The computed trends were interpreted in conjunction with experimental trends in order to establish confidence in the calculated results, and to gain deeper insight into benzotetrazepinone chemistry.

Calculations

All semiempirical calculations were performed with the GAMESS package[34] on a Sun Sparc10 workstation, using RHF wavefunctions. Full geometry optimizations were carried out on each structure in Cartesian (as opposed to internal) coordinates, until the RMS gradient was less than 0.030 kcal mol^{-1} $Å^{-1}$. Transition states and equilibrium geometries were verified as such by force constant analysis, and the correct reactants and products for each transition state were checked by running intrinsic reaction coordinate (IRC) calculations initiated from the transition state in question. Structures and energies varied smoothly throughout all the reaction coordinates. Zero-point vibrational corrections to the reaction energies were not calculated explicitly because these corrections should partially cancel, since the number of vibrational modes is the same in both the reactants and the products in all the intramolecular reactions considered here. Solvent effects were also not considered, because this study is concerned with substituent effects in an intramolecular reaction, where solvent effects should be similar throughout the series of substituted tetrazepinones. Neglecting the solvent should have little effect on the substituent dependent trends.

Results and Discussion

a. Mechanisms of Acid-Induced BTZ Ring Opening to DPMU. Tetrazepinone protonation could occur at either N1, N2, N3, O14, or N5 (Figure 2), but N3 and O14 protonations were considered exclusively, because only these will result in the desired retrosynthetic ring opening. The protonations were assumed reversible and pH dependent, because BTZs precipitate out of the DPMU/BTZ reaction mixture only upon addition of base.

Three pathways for acid-induced BTZ ring opening were considered (Figure 4); in path A, protonation of **1** at N3 forms **5**, which ring-opens through transition state **TS5** to structure **2**. In path B, protonation of **1** at O14 with the hydrogen (*Z*) to N3 forms **6**, which ring-opens through transition state **TS6** to the (*Z*)-enol form of DPMU, structure **8**. Path C is identical to path B, except that the protonating hydrogen is (*E*) instead of (*Z*) to N3. Tautomeric equilibria could exist between the species in the different pathways, as indicated in Figure 4.

PM3 heats of formation (Table 1) for all the structures in Figure 4 were calculated using all the different arylring substituents in Figure 2. Sample reaction coordinates for the path A, path B, and path C mechanisms were constructed from the PM3 energies (Figure 5) by plotting the reaction coordinate versus the relative energy (ΔH_{rel}), computed as

$$\Delta H_{rel} = \Delta Hx - \Delta H_f(H^+) - \Delta H_f(\mathrm{BTZ}) \qquad (1)$$

(5) (a) Stewart, J. J. P. *J. Comput. Chem.* **1989**, *10*, 209. (b) Stewart, J. J. P. *J. Comput. Chem.* **1989**, *10*, 221. (c) Stewart, J. J. P. *J. Comput. Aided Mol. Des.* **1990**, *4*, 1.

(6) Cabre, M.; Farras, J.; Fernandez-Sanz, J.; Vilarrasa, J. *J. Chem. Soc., Perkin Trans. 2* **1990**, 1943.

(7) Fos, E.; Vilarrasa, J.; Fernandez, J. *J. Org. Chem.* **1985**, *50*, 4894.

(8) Palomo, C.; Cossio, F. P.; Cuevas, C.; Lechea, B.; Mieglo, A.; Roman, P.; Luque, A.; Martinez-Ripoll, M. *J. Am. Chem. Soc.* **1992**, *114*, 9360.

(9) Cossio, F. P.; Ugalde, J. M.; Lopez, X.; Lechea, B.; Palomo, C. *J. Am. Chem. Soc.* **1993**, *115*, 995.

(10) Lowe, P. R.; Sansom, C. E.; Schwalbe, C. H.; Stevens, M. F. G.; Clarke, A. S. *J. Med. Chem.* **1992**, *35*, 3377.

(11) Clarke, A. S.; Stevens, M. F. G.; Sansom, C. E.; Schwalbe, C. H. *Anti-Cancer Drug Des.* **1990**, *5*, 63.

(12) Ritchie, J. P. *J. Org. Chem.* **1989**, *54*, 3553.

(13) Mishra, A. K.; Dogra, S. *Indian J. Chem.* **1988**, *27a*, 851.

(14) Mavri, J.; Hadzi, D. *J. Mol. Struct.* **1990**, *224*, 285.

(15) Vernon Cheney, B. *J. Org. Chem.* **1994**, *59*, 773.

(16) de la Concepcion Forces-Forces, M.; Hernandez Cano, F.; Claramunt, R. M.; Sanz, D.; Catalan, J.; Fabero, F.; Fruchier, A.; Elguero, J. *J. Chem. Soc., Perkin Trans. 2* **1990**, 237.

(17) Ozment, J. L.; Schmeidekamp, A. M.; Schultz-Merkel, L. A.; Smith, R. H., Jr.; Michejda, C. J. *J. Am. Chem. Soc.* **1991**, *113*, 397.

(18) Eto, M.; Yoshitake, Y.; Harano, K.; Hisano, T. *J. Chem. Soc., Perkin Trans. 2* **1990**, 1337.

(19) Pop, E.; Huang, M.-J.; Brewster, M. E.; Bodor, N. *J. Mol. Struct. (THEOCHEM)* **1994**, *315* 1.

(20) Barluenga, J.; Sordo, T. L.; Sordo, J. A.; Fustero, S.; Gonzalez, J. *J. Mol. Struct. (THEOCHEM)* **1994**, *315*, 63.

(21) Frau, J.; Donoso, J.; Vilanova, B.; Munoz, F.; Garcia Blanco, F. *Theor. Chim. Acta* **1993**, *86*, 229.

(22) Hotokka, M.; Lonnberg, H. *J. Mol. Struct. (THEOCHEM)* **1996**, *363*, 191.

(23) Jursic, B. S. *J. Mol. Struct. (THEOCHEM)* **1996**, *365*, 55.

(24) Meyer, M. *J. Mol. Struct. (THEOCHEM)* **1994**, *304*, 45.

(25) Williams, C. I. Ph.D. Thesis, McGill University, 1997.

(26) Williams, C. I.; Whitehead, M. A. *J. Mol. Struct. (THEOCHEM)* **1997**, *393*, 9.

(27) Williams, C. I.; Whitehead, M. A.; Jean-Claude, B. J. *J. Mol. Struct. (THEOCHEM)* **1997**, *389*, 13.

(28) Fabian, W. M. F. *Z. Naturforsch.* **1990**, *45a*, 1328.

(29) Jursic, B. S.; Zdravkovski, Z. *J. Mol. Struct. (THEOCHEM)* **1994**, *309*, 241.

(30) Katritzky, A. R.; Yannakopoulou, K.; Anders, E.; Stevens, J.; Szfran, M. *J. Org. Chem.* **1990**, *55*, 5683.

(31) Jursic, B. S.; Zdravkovski, Z. *J. Mol. Struct. (THEOCHEM)* **1994**, *315*, 85.

(32) Ogretir, C.; Yarligan, S. *J. Mol. Struct. (THEOCHEM)* **1996**, *366*, 227.

(33) Williams, C. I.; Whitehead, M. A.; Jean-Claude, B. J. *J. Mol. Struct. (THEOCHEM)* **1997**, *392*, 27.

(34) (a) Schmidt, M. W.; Baldridge, K. K.; Botz, J. A.; Hensen, J. H.; Koseki, S.; Gorden, M. S.; Nguyen, K. A.; Windus, T. L.; Elbert, S. T. *QCPE Bull.* **1990**, *10*, 52. (b) Schmidt, M. W.; Baldridge, K. K.; Botz, J. A.; Elbert, S. T.; Gorden, M. S.; Hensen, J. H.; Koseki, S.; Matsunaga, N.; Nguyen, K. A.; Su, S.; Windus, T. L.; Dupuis, M.; Montgomery, J. A. *J. Comput. Chem.* **1993**, *14*, 1347.

Table 1. PM3 Heats of Formation (kcal/mol)

substituent	1	2	3	5	TS5	6	TS6	7	TS7	8	9	10	TS10	11	TS11	12
a: R = H	47.3	206.3	–	217.8	219.2	213.4	219.3	214.1	221.5	208.4	210.3	206.9	231.8	225.4	234.2	220.1
b: R = *p*OCH_3	9.2	164.3	–	176.6	177.2	174.9	178.4	174.9	179.8	166.7	168.6	–	–	–	–	–
c: R = *p*NO_2	40.9	212.2	–	221.9	224.1	215.6	224.4	216.5	226.1	213.4	215.3	–	–	–	–	–
d: R = *m*Cl	41.2	202.1	–	213.4	214.9	208.5	215.6	209.4	217.2	204.1	206.0	–	–	–	–	–
e: R = *p*Cl	41.1	200.7	–	212.4	–	208.4	–	209.0	–	202.9	204.8	–	–	–	–	–
f: R = *p*F	4.4	166.6	–	177.7	–	173.7	–	174.1	–	168.5	170.4	–	–	–	–	–
g: R = *p*CN	83.9	249.3	–	260.0	–	255.2	–	255.9	–	251.0	252.9	–	–	–	–	–
h: R = *m*OCH_3	9.8	167.6	–	179.3	–	173.9	–	175.2	–	169.9	171.7	–	–	–	–	–
i: R = *m*CH_3	37.9	195.8	–	207.5	–	202.8	–	203.7	–	198.1	199.9	–	–	–	–	–
j: R = *m*NO_2	40.3	210.1	–	220.2	–	215.9	–	216.4	–	211.5	213.6	–	–	–	–	–
k: R = *m*F	4.8	168.3	–	179.2	–	173.9	–	174.9	–	170.1	172.0	–	–	–	–	–
l: pyrido	53.7	210.7	–	227.5	–	221.4	–	221.8	–	218.9	220.2	–	–	–	–	–
m: tricyclic	39.5	195.1	–	208.6	–	205.0	–	205.3	–	203.3	203.4	–	–	–	–	–
n: R(N5) = H	45.2	206.7	–	220.0	–	212.1	217.8	214.6	–	207.2	210.5	199.1	222.5	227.0	234.5	211.6

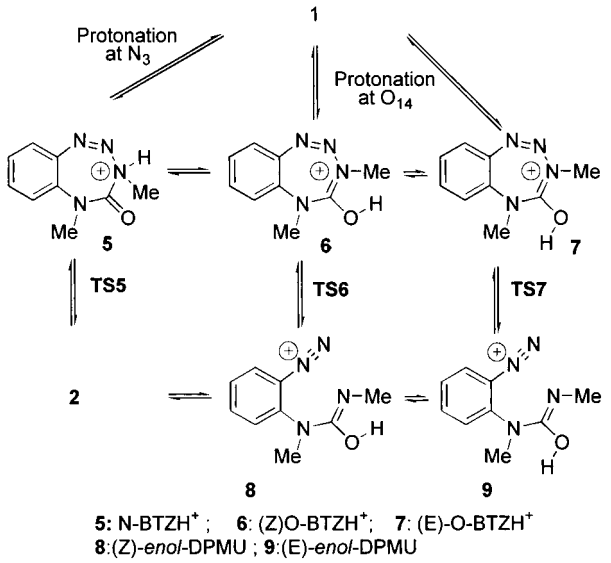

Figure 4. Possible pathways for BTZ ring opening.

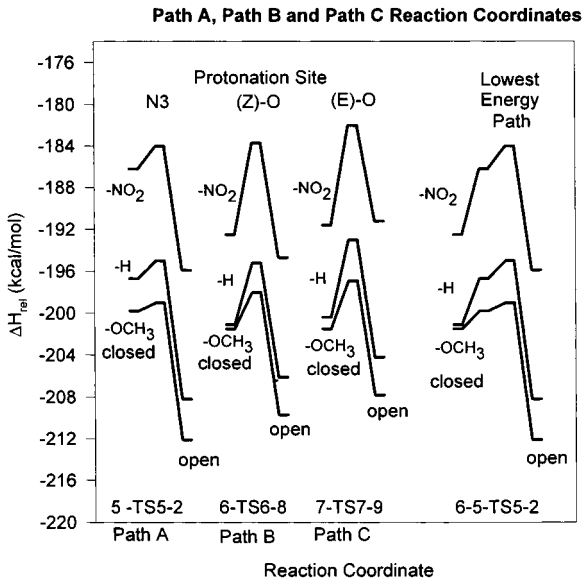

Figure 5. PM3 reaction coordinates for the benzotetrazepinone ring opening mechanisms in Figure 4.

In eq 1, ΔHx is the PM3 heat of formation of the compound in question, ΔH_f(BTZ) is PM3 heat of formation of the unprotonated parent tetrazepinone **1**, and $\Delta H_f(H^+)$ is the experimental H^+ heat of formation (367.2 kcal/mol). Energy barriers to protonation are taken as zero, because the details of the protonation step (although important) were not considered explicitly.

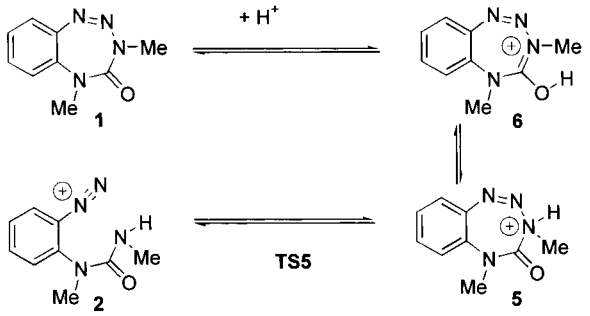

Figure 6. Lowest energy path for acid-induced BTZ ring opening as suggested from PM3 results.

The PM3 energies (Table 1) favor O14 over N3 protonation in BTZs, which is expected because amides and ureas protonate at O as opposed to N.[35] The PM3 energies parallel *ab initio* calculated energies which indicate that O protonation is energetically favored over N3 protonation in structurally analogous (*E*)-formyltriazenes.[36−38]

The lowest energy path for tetrazepinone ring opening (Figure 6) is a combination of paths A and B, where the O-protonated intermediate **6** tautomerizes to the N protonated species **5**, which then ring opens through **TS5** to the keto form of DPMU **2**. However, ring opening of **6** through transition state **TS6** is a feasible alternate path only 0.2−1 kcal/mol higher in energy than the lowest energy pathway. Sample reaction coordinates for the lowest energy path are given in Figure 5.

The experimentally observed effect of aryl-ring substituents on benzotetrazepinone stabilities is clearly demonstrated by the Figure 5 reaction coordinates. Regardless of the actual pathway followed, all reaction coordinates increasingly favor the ring-opened DPMU over the ring-closed protonated BTZ with increasing electron-donating capacity of the aryl ring-substituent.

Optimized Structures. The optimized structures of **2**, **5**, **TS5**, **6**, **TS6**, and **8** will be discussed briefly, but the structures **7**, **TS7**, and **9** will not, because the PM3 energies show that O14 protonation (*Z*) to N3 is always energetically favored over protonation (*E*) to N3 (Table 1).

(35) Zabicky, J., Ed. *The Chemistry of Amides*; John-Wiley & Sons: Toronto, 1970.
(36) Ozment, J. L.; Schmeidekamp, A. M.; Schultz-Merkel, L. A.; Smith, R. H., Jr.; Michejda, C. J. *J. Am. Chem. Soc.* **1991**, *113*, 397.
(37) Schmiedekamp, A. M.; Topol, I. A.; Burt, S. K.; Razafinjanahary, H.; Chermette, H.; Pfaltzgraff, T.; Michejda, C. J. *J. Comput. Chem.* **1994**, *12*, 875.
(38) Kroger-Smith, M. B.; Schmidt, B. F.; Czerwinski, G.; Taneyhill, L. A.; Snyder, E. J.; Kline, A. M.; Michejda, C. J.; Smith, R. H., Jr., *Chem. Res. Toxicol.* **1996**, *9*, 466.

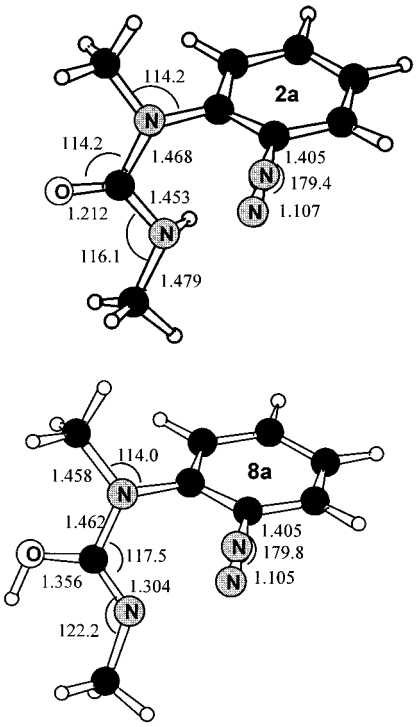

Figure 7. Open-chain DPMU keto and enol forms (all bond lengths in angstroms; all bond angles in degrees).

The PM3 energies favor the keto form of DPMU **2** over the enol forms **7** and **8**, which is expected because unprotonated amides and ureas favor the keto over the enol form.[35] The urea group is almost coplanar within itself in the PM3-optimized **2** and **8** structures (Figure 7), and the urea group is nearly perpendicular to the benzene ring (urea plane/benzene plane torsion angle = 82−88°). The length of the C4−N3 bond in enol−DPMU **8** corresponds to that of an N=C double bond, while the length of the same bond in keto-DPMU **2** corresponds to that of an N−C single bond. The PM3-optimized structure of keto-DPMU **2** is similar to the X-ray structure of (2-aminophenyl)urea, the synthetic precursor of DPMU prior to diazotization.[39,40]

The structures in Figure 8 compare the PM3-optimized geometries of the N3-protonated species **5a**, the O-protonated species **6a**, and unprotonated ground state BTZ **1a**. Protonation of benzotetrazepinones at N3 substantially lengthens the N2−N3 bond (to > 1.8 Å), and Figure 8 demonstrates how the tetrazepinone ring conformation of the N3-protonated species is dissimilar to that of the unprotonated benzotetrazepinone **1a**. *Ab initio* 3-21G* and 6-31G** geometry optimizations were performed on the N3-protonated BTZ structure, but all attempts resulted in a ring opening to the DPMU structure **2**. The instability of the N3-protonated BTZ intermediate **5** toward *ab initio* geometry optimization parallels the results of Smith and other workers,[41,42] who found that *ab initio* geometry optimizations of structurally analogous N3-protonated (*Z*)-triazenes[41,42] and N3-protonated (*Z*)-formyltriazenes[36,37] lengthen the N2−N3 bond to >3 Å. Thus, our *ab initio* results, and those of other workers on similar triazene systems, suggest that the N3-protonated benzotetrazepinone is an unstable species.

In contrast to N3 protonation, O14 protonation of BTZ only slightly lengthens the N2−N3 bond and causes only minor changes to the tetrazepinone ring conformation (structure **6a**, Figure 8). *Ab initio* 3-21G* and 6-31G** geometry optimizations performed on O-protonated BTZs **6a** resulted in cyclic structures similar to the PM3-optimized O-protonated structures.

The PM3-optimized **TS5** and **TS6** transition state structures have identical N2−N3 bond distances (Figure 9); however, like the N3-protonated intermediate, the **TS5** conformation differs substantially from that of the unprotonated BTZ **1**, in a manner analogous to the N3-protonated intermediate. Activation barriers to ring opening of **5** through **TS5** are small (0.5−2 kcal/mol, Table 1), probably because tetrazepinone ring distortion and the lengthened N2−N3 bond in **5** facilitate N2−N3 bond scission. In contrast, the O14-protonated transition state **TS6** is conformationally quite similar to the neutral BTZ (Figures 8 and 9). The O-protonated intermediates **6** have ring-opening activation barriers 3−11 kcal/mol higher than those for the N3-protonated BTZ intermediates **5**, indicating that the O-protonated BTZ is more resistant to ring opening than the N3-protonated intermediate.

Overall, the *ab initio* predictions of an unstable N3-protonated intermediate **5**, and the PM3 prediction of an extended N2−N3 bond length and a low ring-opening activation barrier for the same intermediate, cast doubt upon the existence of the N3-protonated structure. Even if the N3-protonated species does form (possibly through tautomerization), the computational evidence suggests it would be unstable and would quickly ring-open.

b. pH Dependence of Benzotetrazepinone Ring Opening in Acid Media. UV/vis spectral studies of aqueous BTZ solutions show that the diazonium spectral peak increases in intensity with increasing acidity, suggesting that BTZ undergoes a retrosynthetic ring opening to DPMU in aqueous acid. This reaction is analogous to the acid-induced scission of 1,2,3-triazenes.[37] The pH of BTZ ring opening is markedly influenced by the aryl ring substituents.

The PM3 energies and optimized geometries discussed previously suggest that the (*Z*)-O-BTZH$^+$ intermediate **6** and the keto-DPMU **2** are the predominant protonated species in aqueous BTZ acid solution. Thus, the relevant equilibria in acidic BTZ solution can be written in terms of structures **6**, **1**, and **2**, as shown in Figure 10.

Structure **6** behaves like a weak acid in Figure 12, and its K_a can be written in terms of K_{open}

$$K_a = \frac{[\text{BTZ}][\text{H}^+]K_{open}}{[\text{keto-DPMU}]} \quad (2)$$

An expression for the pK_a of **6** can be derived by taking the negative $\log_{10}$ of eq 2.

$$\text{p}K_a = \text{pH} - \log - \log \frac{[\text{BTZ}]}{[\text{keto-DPMU}]} - \log K_{open} \quad (3)$$

Values for K_{open} can be approximated using the PM3 enthalpy difference between structures **2** and **6**, henceforth referred to as $\Delta H_{(2-6)}$.

(39) Jean-Claude, B. J.; Britten, J. F.; Just, G. *Acta Crystallogr. C.* **1993**, *49*, 1070.
(40) Jean-Claude, B. J.; Just, G. *Magn. Reson. Chem.* **1992** *30*, 571.
(41) Smith, R. H., Jr.; Schmeidekamp, A.; Michejda, C. J. *J. Org. Chem.* **1988**, *53*, 3433.
(42) Waldkowski, B. D.; Smith, R. H., Jr.; Michejda, C. J. *J. Am. Chem. Soc.* **1991**, *113*, 7893.

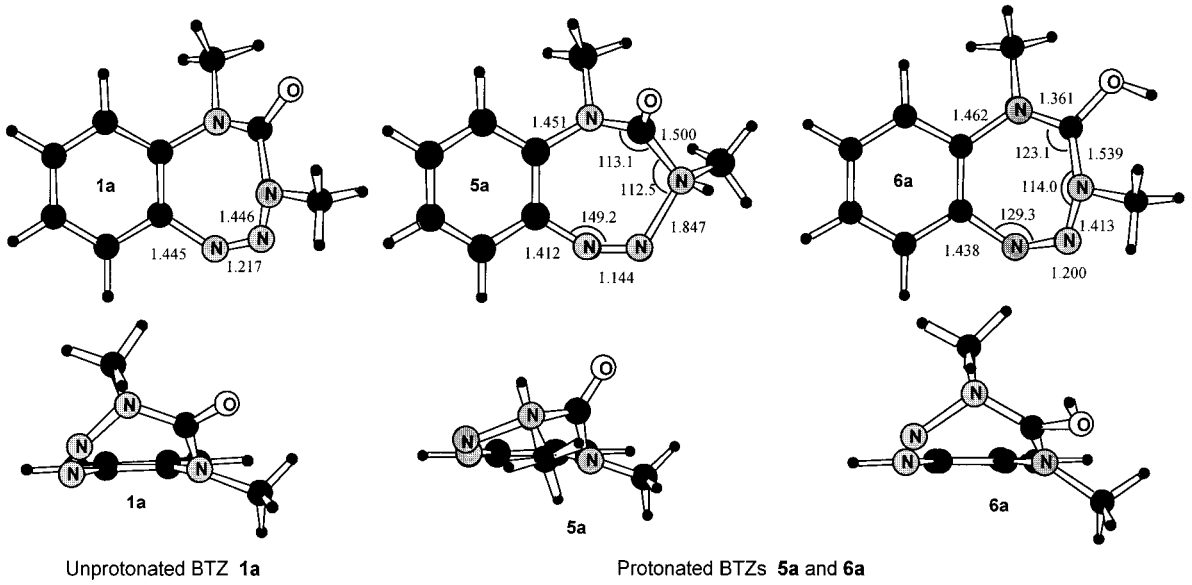

Figure 8. Representative geometries of N3- and O14-promoted BTZs (all bond lengths in angstroms; all bond angles in degrees).

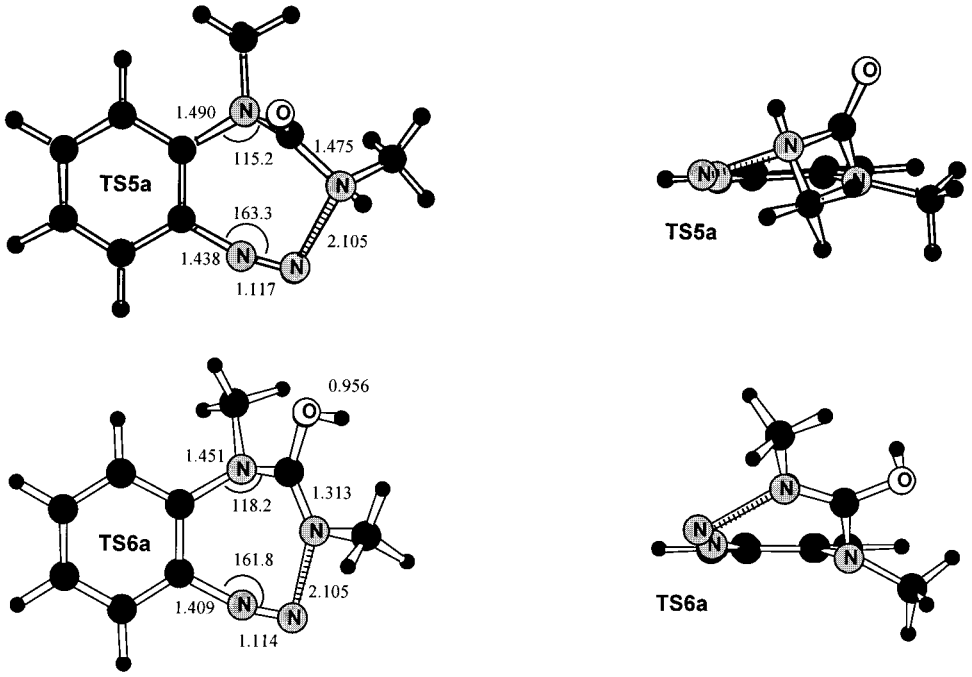

Figure 9. PM3 transition states of N3 and O14 tetrazepinone ring opening (all bond lengths in angstroms; all bond angles in degrees).

$$\Delta H_{(\mathbf{2}-\mathbf{6})} \approx -RT \ln K_{\text{open}} \quad (4)$$

Entropy is ignored in eq 4 because the ring-opening is an intramolecular reaction, and the effect of entropy should be constant throughout the series of compounds. By defining $\Delta\text{pH} = (\text{pH} - \text{p}K_a)$, the [BTZ]/[keto-DPMU] ratio in eq 3 can be related to ΔpH using

$$\Delta\text{pH} - \log K_{\text{open}} = \log [\text{BTZ}]/[\text{keto-DPMU}] \quad (5)$$

Equation (5) can be evaluated using PM3 values of K_{open} from eq 4. The effect of ΔpH on BTZ ring opening was determined for compounds **1a** and **1c** by plotting the [BTZ]/[keto-DPMU] ratio as a function of ΔpH (Figure 11).

The calculated ΔpH curves can be compared with experimental points obtained from UV/vis spectra[3] by plotting the experimental pH points as pH = ΔpH. The experimental pK_a of (*Z*)-O-BTZH$^+$ is unknown, but a pK_a value of −1.0 was chosen to maximized coincidence between the computed and the experimental plots. For simplicity, the same pK_a value was assumed for the unsubstitiuted **1a** and *p* nitro **1c** tetrazepinones.

Despite their differences, the experimental and calculated points in Figure 11 both demonstrate the same effect of aryl ring substituents on the pH of BTZ ring opening. Deviations between the experimental and computed points probably arise because the computed points neglect solvent effects, assume the same pK_a for both **6a** and **6c**, and consider only one possible decomposition mechanism. In addition, the experimental points in Figure 11 are of low quality, because only a handful of these experiments have been performed, and accurate

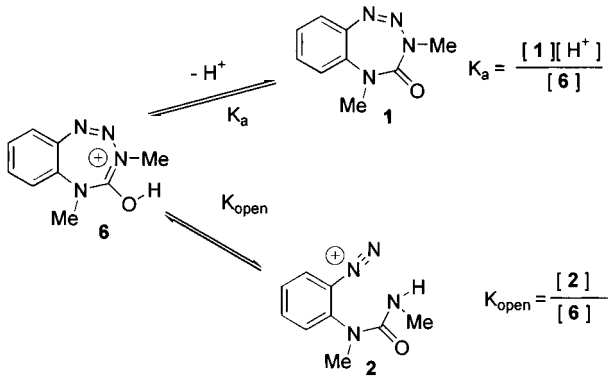

Figure 10. Equilibria in acidic BTZ solution.

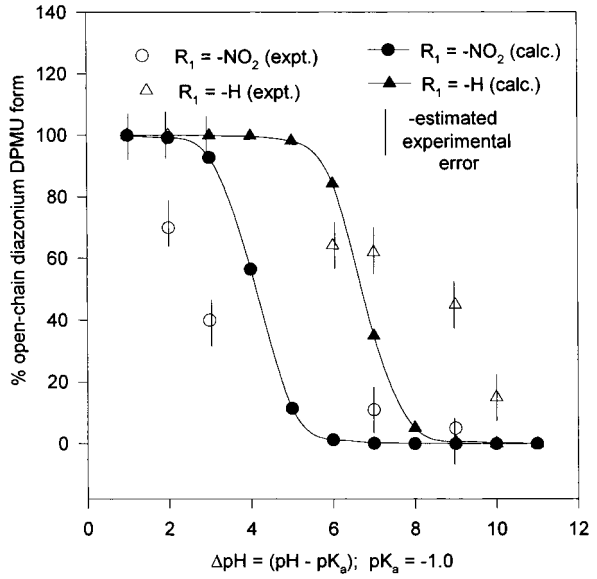

Figure 11. Comparison of experimental and calculated pH dependence of benzotetrazepinone ring opening.

determination of the DPMU concentration is made difficult by the small and broad UV/vis diazonium spectral peak used in its assay. However, there is sufficient correlation between the calculated and experimental trends to lend confidence to the computational results.

The calculated plots in Figure 11 can be used to extract estimates of protonated benzotetrazepinone pK_a's. As mentioned previously, a pK_a of −1.0 was chosen to maximize correlation between the calculated and experimental plots in Figure 11; this suggests that (*Z*)-O-BTZH+ (structure **6**) has a the pK_a value near −1.0. This is a reasonable pK_a value, and may well be expected, because protonated benzamides and phenylureas (which are similar in structure to DPMU and BTZ) have experimental pK_a values between −1.0 to −3.3.[35]

c. Hammett Correlation of Substituent Effects in DPMU Ring Closures. Hammett linear free energy relationships (LFER) are often used in experimental physical chemistry to quantitatively measure reactivity as a function of aryl-ring substituents.[43] Ring-closure of DPMU to BTZs is analogous to many other diazo coupling reactions,[44−46] some of which follow Hammett-like

Table 2. Hammett Constants and Calculated log *K′/K*

aryl-ring substituent R	Δ*H* (**6**−**2**) (kcal/mol)	log *K′/K*	σ [a]	σ^+ [a]
a: R = H	7.1	0	0	0
b: R = *p*OCH$_3$	10.6	−2.55	−0.27	−0.78
c: R = *p*NO$_2$	3.4	2.69	0.78	0.79
d: R = *m*Cl	6.4	0.51	0.37	0.40
e: R = *p*Cl	7.7	−0.43	0.23	0.11
f: R = *p*F	7.1	0	0.06	−0.07
g: R = *p*CN	5.9	0.87	0.66	0.66
h: R = *m*OCH$_3$	6.3	0.58	0.12	0.05
i: R = *m*CH$_3$	7.0	0.07	−0.07	−0.07
j: R = mNO$_2$	5.8	0.94	0.71	0.67
k: R = *m*F	5.6	1.09	0.34	0.35

[a] Values of σ and σ^+ taken from ref 47.

LFERs.[46] Thus, the Hammett[43]

$$\rho\sigma = \log \frac{K'}{K} \qquad (6)$$

and the modified Hammett

$$\rho^+\sigma^+ = \log \frac{K'}{K} \qquad (7)$$

equations were used to measure the aryl-ring substituent dependence of DPMU ring-closure to BTZ. The Hammett and modified Hammett constants σ and σ^+ in eqs 6 and 7 describe the electron-donating/electron-withdrawing capacity of the aryl-ring substituents.[43] The magnitude and sign of the reaction constants ρ and ρ^+ quantify the sensitivity of the reaction toward aryl-ring substitutents and can be used to extract qualitative information about the reactant, product, and transition state structures. In eqs 6 and 7, *K′* is the ring closure equilibrium constant K_{close} for the substituted DPMU ring closure, while *K* is K_{close} for the unsubstituted DPMU ring closure. Since the ring closure equilibrium is simply the reverse of the ring opening equilibrium between **6** and **2** in Figure 10, $K_{close} = 1/K_{open}$, and values of log *K′/K* can be calculated using eq 4 and PM3 $\Delta H_{(\mathbf{6}-\mathbf{2})}$ enthalpy differences and

$$(\mathrm{u}\Delta H_{(\mathbf{6}-\mathbf{2})} - \mathrm{s}\Delta H_{(\mathbf{6}-\mathbf{2})})/(2.303RT) = \log \frac{K'}{K} \qquad (8)$$

The s- and u-prefixes in eq 8 specify the "substituted" and "unsubstituted" **6** → **2** enthalpy differences, respectively. Equation 8 was evaluated for all the aryl-ring-substituted benzotetrazepinones in Figure 2 (**a**−**k**), with the temperature arbitrarily set at 300 K (Table 2). The respective Hammett eqs 6 and 7 were plotted (Figure 12, plots a and b) using σ and $\sigma+$ values from ref 47.

Although there is some scatter in the Figure 12 plots, both plots clearly show a Hammett like behavior of the ring closure reaction. Reaction constants of $\rho = +3.26$ and $\rho+ = +2.55$ were calculated by linear regression analysis of the data. The reaction constants ρ and $\rho+$ are both positive, which is consistent with a reaction whose rate is increased by electron withdrawal. The relatively large ρ and $\rho+$ values are consistent with a highly substituent dependent reaction. In addition, the

(43) (a) Issacs, N. S. *Physical Organic Chemistry*; John Wiley and Sons: New York, 1987. (b) Lowry, T. H.; Richardson, K. S. *Mechanism and Theory in Organic Chemistry*; Harper-Row: New York; 1976. (c) Pross, A. *Theoretical and Physical Principles of Organic Reactivity*; Wiley: New York; 1995.

(44) Saunders, K. H.; Allen, R. L. M. *Aromatic Diazo Compounds*; Edward Arnold: London; 1985.

(45) Zollinger, H. *Azo and Diazo Chemistry; Aliphatic and Aromatic Compounds*; Interscience: New York, 1961.

(46) Zollinger, H. *Azo and Diazo Chemistry I: Aromatic and Heterocyclic*; VCH: New York, 1995.

(47) Dean, J. A., Ed. *Lange's Handbook of Chemistry*, 14th ed.; McGraw-Hill: New York, 1992.

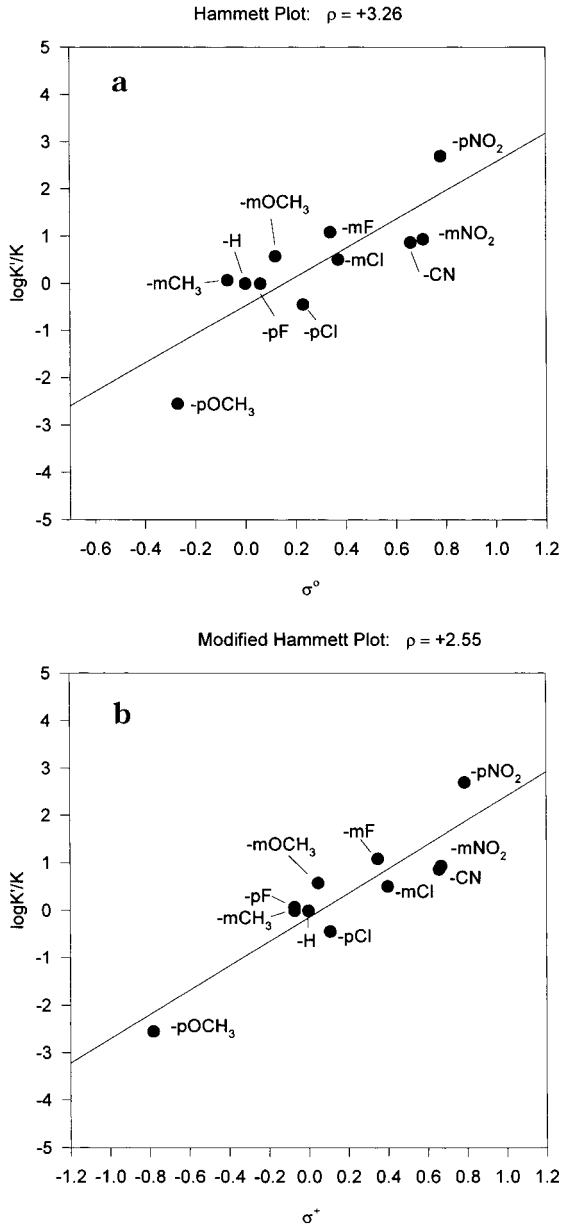

Figure 12. (a) Hammett plot for DPMU ring closure. (b) Modified Hammett plot (σ^+) of DPMU ring closure.

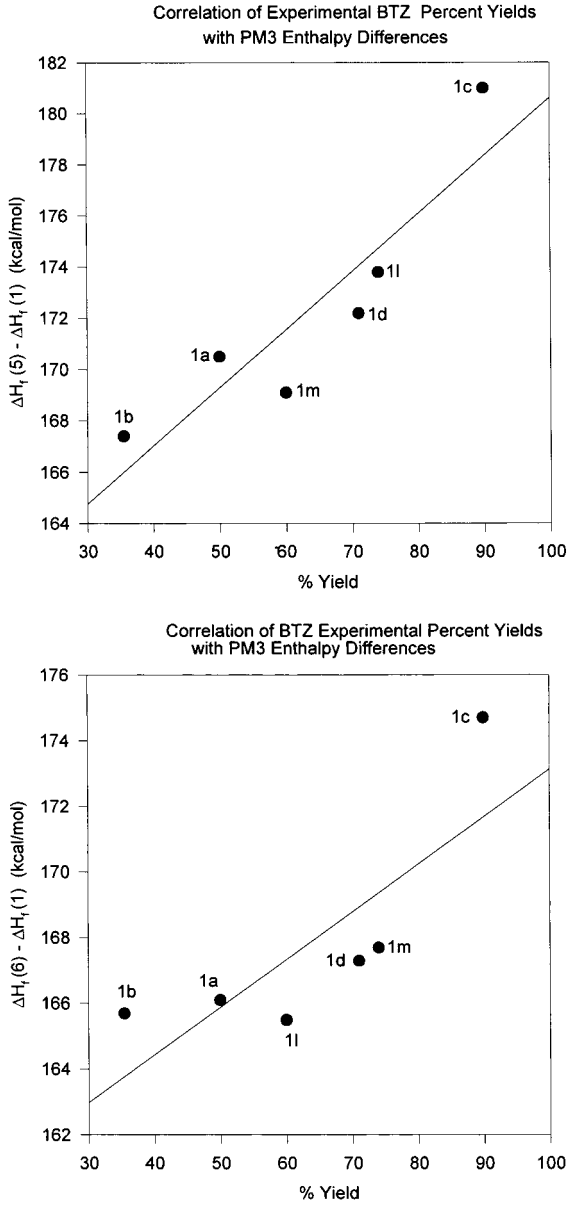

Figure 13. (a) **5**−**1** relative enthalpy difference vs percent yield. (b) **6**−**1** relative enthalpy difference vs percent yield.

calculated reaction constants are similar to experimentally determined reaction constants of other diazo coupling reactions.[45,46] Standard errors of 0.708 and 0.427 for ρ and $\rho+$, respectively, indicate a better fit between the PM3 data and the $\sigma+$ substituent constants, which is expected because $\sigma+$ substituent constants are more appropriate for diazonium coupling reactions, where a formal positive charge is directly bonded to the aryl ring.[43]

d. Substituent Effects in BTZ Experimental Percentage Yields. A semiquantitative relationship can be obtained by correlating experimental tetrazepinone percent yields with PM3 enthalpy differences. The $\Delta H_{rxn(5-1)}$ and $\Delta H_{rxn(6-1)}$ enthalpy differences (Figure 13b) both correlate linearly with the experimental yields, although there is better correlation with the $\Delta H_{rxn(5-1)}$ enthalpy differences (Figure 13a). While there is no extensive theoretical justification for these correlations, they may be useful as a rough guide for practical synthesis.

e. Cyclization of DPMU to *N*-Carbamoylbenzotriazoles (NCBT). DPMUs with R = CH_3 as the N5 substituent never internally cyclize at N5, and the *N*-carbamoylbenzotriazole (NCBT) product is never obtained in these reactions. However, attempts to synthesize BTZ with R = H as an N5 substituent fail, because the DPMU cyclizes at N5 instead of N3, and the NCBT product is formed exclusively (Figure 1).[3] The two mechanisms proposed to explain these reaction, outlined in Figure 14, are (a) the keto-path, where cyclization of the keto-DPMU **2** at N5 through transition state **TS11** forms the protonated species **11f** (if R = H), or the quaternary N^+ species **11a** (if R = Me); and (b) the enol-path, where the enol form of DPMU **10** undergoes cyclization through **TS10** to the O-protonated (or methylated) *N*-carbamoylbenzotriazole **12**.

PM3 heats of formation for the species in Figure 14 were calculated (Table 1) with both R = H and R = CH_3 as the N5 substituent. Reaction coordinates for the enol- and keto-paths were constructed using the PM3 heats of formation (Figure 15). The reaction coordinates for the ring closure of enol-DPMU to (*Z*)-O-BTZH$^+$ are also included in Figure 15, to compare the ring closure to NCBT with the ring closure to BTZ.

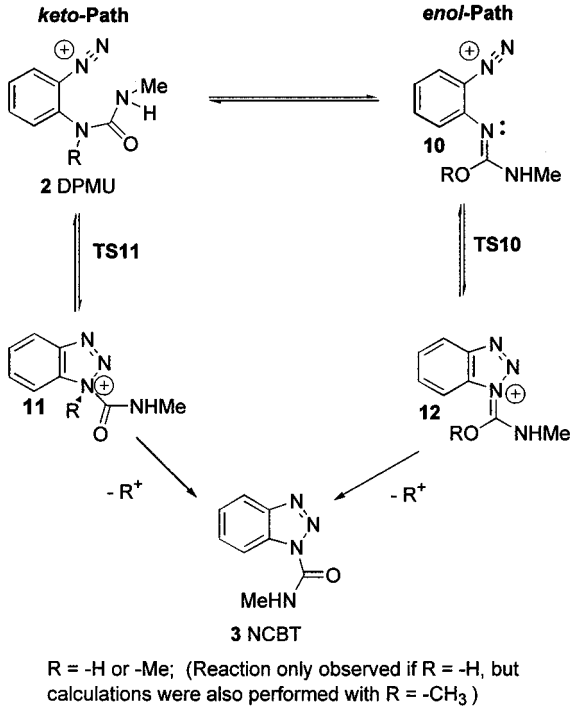

Figure 14. Proposed mechanisms for ring closure of DPMU to NCBTs.

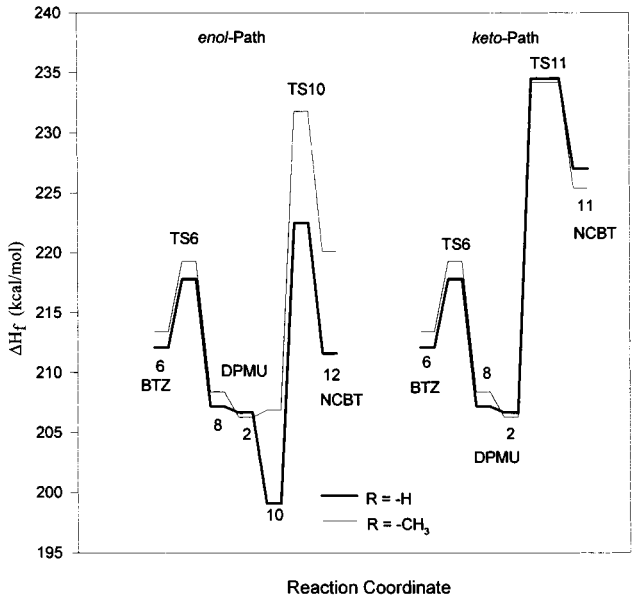

Figure 15. Reaction coordinates for enol- and keto-paths for DPMU → NCBT ring closure.

The Figure 15 reaction coordinate shows that the energies in the keto-path are almost identical, regardless of whether the N5 substituent is R = CH_3 or R = H. Formation of the protonated (*Z*)-O-BTZH$^+$ intermediate (structure **6**) is favored over formation of the **11** type structure, presumably because of strain effects in the **11** type intermediate. PM3-optimized geometries of both **11a** and **11n** show elongated N2−N5 bond distances (>1.8 Å), similar to the elongated N2−N3 bonds in N-BTZH$^+$ **5** intermediates. In addition, transition state barriers for the ring closure of DPMUs to **11** type structures are substantially higher than those for ring closure to BTZ. Overall, the keto-path reaction coordinate suggests that if the keto- path were followed exclusively, the R = H and R = CH_3 N5-substituted DPMUs would both cyclize to BTZs with similar synthetic percent yields. The keto-path does not account for the experimentally observed cyclization of DPMU to NCBT with H as the N5 substituent, and therefore, this path is probably not the mechanism by which DPMU cyclizes to NCBT.

Table 3. *Ab Initio* Energies Used in This Study

structure	*ab initio* total energy (au) 3-21G*	*ab initio* total energy (au) 3-21G*//6-31G** [b]	PM3 energy differences (kcal/mol)
2a	−636.03714	−636.63926	206.3
10a	−636.03683	−636.64016	206.9
Δ*E* (**10a**−**2a**) (kcal/mol)[a]	0.19	0.56	0.6
2n	−597.22132	−600.61002	206.7
10n	−597.22175	−600.61506	199.1
Δ*E* (**10n**−**2n**) (kcal/mol)[a]	−0.27	−3.16	−7.6

[a] 1 au = 627.51 kcal/mol. [b] 6-31G** single point calculations performed at the 3-21G*-optimized geometry.

Further evidence that the keto path is not the mechanism of ring closure to NCBT comes from *ab initio* calculations. *Ab initio* (3-21G*, 6-31G**) geometry optimizations of structures **11a** and **11n** result in a lengthening of the N2−N5 bond to >3 Å. Thus, these *ab initio* calculations predict that the **11** type species are unstable. This result is analogous to the previously discussed *ab initio* geometry optimizations of the N3-protonated tetrazepinones. The elongated N2−N5 bonds in the PM3-optimized **11a** and **11n** structures and the *ab initio* predictions of unstable **11** type structures cast doubt upon the existence of **11** type intermediates as stable species, and the ability of DPMU to cyclize to NCBT by the keto-path.

In contrast to the keto path, there is a striking difference between the R = CH_3 and R = H enol-path reaction coordinates in Figure 15. Surprisingly, PM3 predicts that the enol-DPMU **10n** is more stable than the corresponding keto-DPMU form **2n**, while the enol-DPMU **10a** is less stable than the corresponding keto-DPMU **2a**. This PM3 result is verified by 3-21G* and 3-21G*//6-31G** *ab initio* calculations performed on structures **2a**, **2n**, **10a** and **10n** (Table 3). With H as the N5 substituent, both PM3 and *ab initio* predict that the enol form **10n** is more stable than the keto form **2n**, while with Me as the N5 substituent, the reverse is true.

The large difference in the stabilities of **10** as a function of the N5 substituent can be explained by considering the structural differences between **10a** and **10n** (Figure 16). The bond lengths and angles are almost identical in both **10n** (R = H) and **10a** (R = CH_3). However, the side-chain in **10n** is coplanar with the benzene ring, and therefore, the enhanced stability of this species is probably due to conjugation with the benzene ring. The planar geometry of **10n** also facilitates ring closure to the planar O-protonated NCBT **12n** species.

The reaction coordinate in Figure 15 shows that **12n** has a stability similar to that of (*Z*)-O-BTZH$^+$ **6n**. This suggests that an equal mixture of NCBT and BTZ should be obtained when DPMUs with R = H cyclize. In addition, cyclization of enol-DPMU **10n** with R = H to O-protonated NCBT occurs through a relatively large activation energy barrier. This further suggests that little or no NCBT **12n** will form. However, although the activation barrier is high, proton loss from O-protonated NCBT **12n** is irreversible because addition of base is

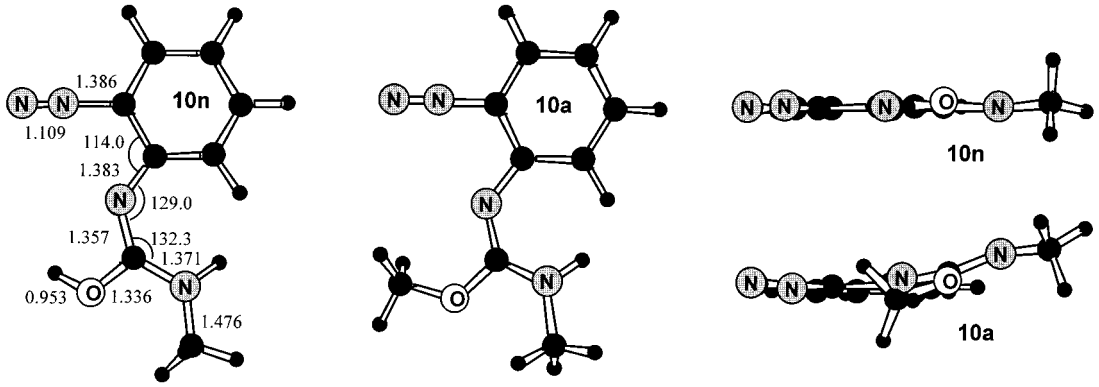

Figure 16. PM3-optimized structures of **10n** and **10a**.

unnecessary to precipitate NCBT from the synthetic reaction mixture. This irreversible proton loss from **12n** drives the reaction **10n** → **12n** toward the *N*-carbamoylbenzotriazole product NCBT **3n**. Thus, NCBT is the only product obtained from internal cyclization of DPMU **2n**.

In contrast to **10n**, the side-chain in the R = CH_3 **10a** species is 11.2° out-of-plane with the benzene ring, probably because the methyl group prevents rotation of the side-chain into the aromatic ring plane. The stability of **10a** is not enhanced by resonance, and the orientation of the side-chain in hinders ring closure to *O*-methoxy NCBT **12a**. The *O*-methoxy NCBT **12a** is much less stable than the corresponding (*Z*)-O-BTZH$^+$ **6a** for DPMU with R = CH_3, explaining why only BTZs are produced from cyclizations of DPMU with N5 substituents R = CH_3. The enol form of DPMU is more stable than the keto form only when R = H. Thus, cyclization of enol-DPMU to O-protonated NCBT is only possible when R = H; when R = CH_3 cyclization to NCBT is not favored, cyclization to BTZ occurs instead.

Conclusions

The PM3 semiempirical method was used to successfully study the acid induced ring-opening of benzotetrazepinones (BTZs). The results indicate that BTZ most likely protonates at O as opposed to N3 and that ring-opening could occur from either an O or N3-protonated species. Protonated BTZ pK_a's (pK_a = −1.0) were estimated by comparing the PM3 results with the experimentally determined pH dependence of BTZ ring opening. The PM3 energies of DPMU ring-closures to BTZs show a Hammett like aryl ring substituent dependence. The PM3 energies were used to determine LFER reaction constants (ρ and ρ+) which support the proposed mechanism and are consistent with experimentally determined reaction constants for similar intramolecular diazo-coupling reactions.[35,46] PM3 enthalpy differences were semiquantitatively related to BTZ experimental percent yields. The mechanism proposed in Figure 4 and the subsequent PM3 calculations are consistent with all experimental observations. The PM3 method was also used to explain why NCBT, and not BTZ, is produced from internal cyclization of DPMU with R = H (instead of R = CH_3) as the N5 substituent.

This work shows that the PM3 method is reasonable to study the acid-induced decomposition mechanisms of benzotetrazepinones. The results for the PM3 method applied to other diazo coupling reactions, and benzotetrazepinone decomposition reactions will be published shortly.

Acknowledgment. C. I. Williams would like to thank the National Sciences and Engineering Research Council of Canada (NSERC) for supporting this research. B. J. Jean-Claude would like to thank the National Cancer Institute of Canada (NCIC) and the Luigi Berba Funds for financial support.

JO9702251